available at www.sciencedirect.com

ScienceDirect

journal homepage: www.elsevier.com/locate/ecolmodel

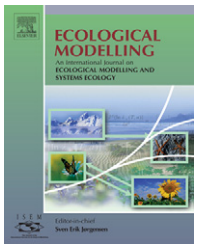

Modification of an ecosystem model for filling medium-sized gaps in tower-based estimates of net ecosystem productivity

Zisheng Xing[a,e], *Charles P.-A. Bourque*[a,b,*], *Fan-Rui Meng*[a], *Roger M. Cox*[c], *D. Edwin Swift*[c], *Tianshan Zha*[d], *Lien Chow*[e]

[a] *Faculty of Forestry and Environmental Management, University of New Brunswick, Fredericton, New Brunswick, Canada E3B 6C2*

[b] *Lanzhou Regional Climate Centre, 2070 Donggang East Road, Lanzhou 730020, Gansu, PR China*

[c] *Natural Resources Canada, Canadian Forest Service, Atlantic Forestry Centre, P.O. Box 4000, Fredericton, New Brunswick, Canada E3B 5P7*

[d] *Climate Research Branch, Environment Canada, 11 Innovation RD, Saskatoon, Saskatchewan, Canada S7N 3H5*

[e] *Potato Research Centre, 850 Lincoln Road, P.O. Box 20280, Fredericton, New Brunswick, Canada E3B 4Z7*

ARTICLE INFO

Article history:
Received 15 March 2007
Received in revised form
26 November 2007
Accepted 29 November 2007
Published on line 16 January 2008

Keywords:
Air temperature modifier
Ecosystem respiration
Gap filling
Net ecosystem productivity

ABSTRACT

Gap filling of flux data is necessary to assist with periodic interruptions in the measurement data stream. The gap-filling model (GFM), first described in Xing et al. [Xing, Z., Bourque, C.P.-A., Meng, F.-R., Zha, T.-S., Cox, R.M., Swift, E., 2007. A simple net ecosystem productivity model for gap filling of tower-based fluxes: an extension of Landsberg's equation with modifications to the light interception term. Ecol. Model. 206, 250–262], was modified to account for the day-to-day control of net ecosystem productivity (NEP) by incorporating air and soil temperature as new controlling variables in the calculation of NEP. To account for the multiple-phase influences of air and soil temperature on plant growth we model ecosystem respiration as a function of soil and canopy respiration. The paper presents model development in an incremental fashion in order to quantify the contribution of individual model enhancements to the prediction of NEP during periods when air and soil temperature variations are important.

Model efficiency (ME) was used to compare the performance of the various forms of the GFM under several combinations of weather conditions during a 34-day period. Results from model comparisons illustrated that the models displayed reasonable performance (ME = 0.75–0.95), with the final GFM displaying the best overall performance. Further evaluation of the final GFM was conducted by comparing the NEP-model results with results generated with an alternative gap-filling approach espoused by Fluxnet-Canada Research Network (FCRN). These evaluations are based on the same 34-day dataset as used in the initial model comparison. Both gap-filling methodologies performed well, but some level of disagreement was present.

* *Corresponding author at*: Faculty of Forestry and Environmental Management, University of New Brunswick, Fredericton, New Brunswick, Canada E3B 6C2. Tel.: +1 506 453 4930; fax: +1 506 453 3538.
E-mail address: cbourque@unb.ca (C.P.-A. Bourque).

0304-3800/$ – see front matter © 2007 Elsevier B.V. All rights reserved.
doi:10.1016/j.ecolmodel.2007.11.019

1. Introduction

Gaps (due to data missing or rejected for quality reasons) in eddy covariance-based measurements are common. These gaps potentially bias calculations of NEP, as in other flux-based variables such as sensible and latent heat. Data gaps need to be filled in order to derive annual sums or to simply analyze temporal trends in the data. In previous work, Xing et al. (2007) developed a gap-filling model (GFM) that takes into account the non-uniform influence of available photosynthetically active radiation (typically with a response time of a few minutes to hours) within stratified plant canopies to improve the quality of gap filling. However, air and soil temperature, which tend to vary at a lower frequency also have their influence on NEP (with a response time of a few hours to a day). To properly model gaps in NEP data lasting more than a few hours to a day, temperature influences on NEP need addressing.

Controversy exists as to the degree temperature controls net ecosystem productivity (NEP). Chen et al. (2002) found that air temperature had no significant influence on NEP in old-growth forests, but demonstrated greater influence in younger forests. Bassow and Bazzaz (1998) suggested that air temperature explained approximately 12% of the photosynthetic variation in red oak (*Quercus rubra* L.), 16% in yellow birch (*Betula alleghaniensis* Britt), and to a lower degree in white birch (*Betula papyrifera*). They also found that air temperature was only weakly correlated with photosynthesis during the summer, but had a higher correlation in September for many tree species. After a thorough review of 27 scientific articles on this subject, Saxe et al. (2001) concluded that high temperatures increased the rate of carbon dioxide (CO_2) absorption to an optimum, but the extent of this increase depended on ambient temperatures. Air temperatures higher than optimum tend to cause a reduction in CO_2 uptake.

As Bassow and Bazzaz's (1998) path analysis[1] indicated, air temperature may impact photosynthesis in both direct and indirect ways. Temperature has been shown to directly affect photosynthesis by affecting (i) photosynthetic chemical reactions, (ii) photochemical efficiency of PSII,[2] and (iii) photo-inhibition. Temperature may indirectly affect photosynthesis by altering (i) pigment content in leaves, (ii) apparent quantum yields, and (iii) respiration rates, by modifying secondary environmental-growth controls, such as water vapor pressure deficit (VPD), nutrient availability, and associated bio-geochemical interactions in soils. This dependence on temperature is well documented (e.g., McMurtrie and Wang, 1993; Hollinger et al., 1999; Cai and Dang, 2002; Leuning, 2002), although mechanisms for this dependence may vary from time to time depending on prevailing meteorological and site conditions.

Grant et al. (2005) found that high air temperatures adversely affected NEP in temperate and boreal coniferous forests by increasing respiration. Model results generated by Grant et al. (2001) predicted that black spruce forests in the boreal region of Canada would change from a CO_2 sink to a CO_2 source with an increase in daily minimum and maximum temperatures above 15 and 25 °C, respectively. Above-average temperatures in British Columbia in 1998 were found to increase annual respiration in temperate coastal Douglas fir forests, which caused a reduction in annual NEP (Morgenstern et al., 2004). Temperature influences on regional estimates of NEP also depend on in situ conditions, such as forest species composition, stand age, and interannual climate variation.

Currently, there are two ways to incorporate air temperature effects in NEP models. One way is to use temperature as a modifier of stomatal conductance either at the canopy or the leaf level (Jarvis and McNaughton, 1986; Leuning, 1995). The second way is to use air temperature as a modifier of maximum quantum efficiencies and related parameters (Farquhar, 1980; Harley and Baldocchi, 1995; Leuning et al., 1998; Chen et al., 1999; Caemmerer, 2000). Traditionally, the modifier is treated as an Arrhenius function—a polynomial function of air temperature. This function has been broadly used in ecosystem models such as *ecosys* (Grant, 2004), CLASS (Verseghy, 1991, 2000; Verseghy et al., 1991), and ecological assimilation of climate and land observation (EALCO). However, as Grant et al. (2005) point out, the Arrhenius function performs "too gradually" in some cases, or "too abruptly" in others, because the function cannot be easily adjusted to account for the effects of other key environmental controls.

In relation to assessing NEP, ecosystem respiration is often problematic because of the difficulty and uncertainty associated with its determination. Soil respiration, a significant component of ecosystem respiration, is critical to nighttime NEP (Zha et al., 2007). Although soil respiration is highly regulated by soil temperature (Lloyd and Taylor, 1994; Gu et al., 1999; Coleman et al., 2002; Lavigne, 2003), recent modelling and experimental investigations by Liu and Edwards (2006) have identified several non-soil temperature controls on soil respiration (e.g., soil water content and soil texture). Lavigne (2003) demonstrated that the Q_{10}[3] parameter may vary with year, soil temperature category, and weather zonation; most likely as an outcome of variations in these non-soil temperature controls.

Soil temperature is considered as an important variable in soil bio-geochemical processes (Kimmins, 1987) as temperature controls (i) the activity of roots and soil organisms, (ii) rates of decomposition, and (iii) nutrient uptake and release and subsequently controls the amount of CO_2 produced in soils by autotrophic and heterotrophic processes. However, the transportation of CO_2 gas in soils is very much regulated by the surface condition of the soil complex and prevailing weather conditions. For example, heavy rain may cause pooling of water over the soil complex effectively blocking the release

[1] Path analysis is a method of "decomposing and interpreting linear relationships among a set of variables by assuming that (1) a weak causal order among these variables is known and (2) the relationships among these variables are causally closed". Path analysis may be viewed as "a method of working out the logical consequences" of these two assumptions.

[2] PSII = photosystem II, which absorbs a shorter wavelength of light (680 nm).

[3] $Q_{10} = e^{10B(1/T/T_{opt})}$, defines the respiration rate for a 10 °C increase in temperature and serves as a parameter in the soil respiration function, $SR = R_{10}Q_{10}^{(T-T_{opt})/T_{opt}}$, where R_{10} is an equation parameter, T is soil temperature, and T_{opt} is a reference temperature.

of CO_2, or strong overhead winds may assist in the release of soil CO_2 by enhancing surface ventilation and increasing diffusion of CO_2 at the air–surface (canopy) interface. Furthermore, water content in the litter layer or in the organic layer in soils may impose added complexities to the modelling of soil respiration. Exponential treatment of soil respiration (Lloyd and Taylor, 1994; Gu et al., 1999; Lavigne, 2003) could potentially generate excellent predictions over long time intervals, but not so at shorter (e.g., sub-hour) time intervals.

The objectives of this research are to (i) further refine the GFM developed by Xing et al. (2007) by incorporating (a) a modifier that adjusts maximum growth according to air temperature, and (b) an ecosystem respiration term that uses soil temperature as the main control on soil respiration; (ii) study the relative impact of these enhancements on the calculation of NEP; (iii) evaluate the performance of the resultant model with various combinations of environmental conditions; and (iv) assess the applicability of the model in gap filling of NEP data.

2. Materials and methods

2.1. Research site and measurements

The research forest site, from which all NEP and micrometeorological data in this paper originated, is predominantly composed of balsam fir (*Abies balsamea* (L.) Mill; BF) and is located about 1 km east of *Nashwaak Lake* (NWL_BF) in the Central Uplands eco-region (Ecological Classification Working Group—ECWG, 2003) of New Brunswick (NB; 46°28′20″N, 67°06′0″W) distinguished by its warm, rainy summers and mild, snowy winters. The research site is in hilly terrain with elevations ranging from 320 to 350 m. Mean annual air temperature for the growing season is 10.8 °C. The mean annual rainfall is 1392 mm. The average number of growing degree-days for this region is about 1302 °C. The soil is a generally well-drained sandy loam, with an average duff thickness of 6–7 cm. The site is very rocky with some large boulders interspersed. Mixed wood forests in the region are primarily composed of sugar and red maple (*Acer saccharum* Marsh., *Acer rubrum* L.; SM and RM), red and white spruce (*Picea rubens* Sarg., *Picea glauca* [Moench] Voss; RS and WS), and BF. At the site, BF makes up for more than 95% of the total site volume (Xing et al., 2005; Table 1).

At the research site, a 20-m high triangular tower was used to host a series of eddy-covariance sensors to collect high-frequency (10 Hz) measurements of water vapor and CO_2 concentrations, horizontal, lateral, and vertical wind velocities, and air temperatures. Eddy-covariance sensors were placed above the forest canopy (at 13.5 m height; Table 1) at a height of about 16.5 m above ground. The eddy-covariance sensors included a close path infra-red gas analyzer (IRGA, LI-7000, Li-COR, Lincoln, Nebraska) placed in a thermostatically controlled "white" box (courtesy of the Biometeorology and Soil Physics Group of the University of British Columbia), a 3-dimensional (u, v and w) sonic anemometer [CSAT3, Campbell Scientific (Canada), Edmonton, Alberta], and a fine-wire thermocouple. Meteorological sensors on the tower included a series of photosynthetically active radiation (PAR) sensors (LI-190SA, Li-COR, Lincoln, Nebraska), a series of temperature and relative humidity sensors (5 HMP45C T-RH probes; CSC) placed at regular intervals along the length of the tower, and a CNR1 net radiation sensor (CSC) installed 5 m above the forest canopy. Ancillary site information collected included soil temperature (using a series of 107 thermisters; CSC) and soil moisture (CS616; CSC) profiles (2, 5, 10, 20, 50 cm deep from the soil surface) in two separate pits about 5–7 m west to northwest of the flux tower. All information was recorded on a CR5000 datalogger (CSC). For additional information on tower and equipment set-up, sensor calibration, and maintenance schedules refer to Coursolle et al. (2006).

NEP fluxes were calculated from the mean covariance between the vertical wind speed and the CO_2 mixing ratios

Table 1 – NWL_BF site characteristics

Site descriptor	Parameters
Location	46°28′20″N and 67°06′00″W
Stand size (ha)	31
Stand composition[a] (%)	95% BF, 5% BS, WB, TA
Average stand slope (at the tower (°)	4.1 ± 0.7[b] (3.7)
Stand age (years)	32–37
Management intervention applied, year of application	PCT[b], started in 1981 and finished in 1985
Residual after PCT (stems ha^{-1})	2250
Mean tree height (m)	13.5
Mean diameter at breast height (cm)	12.9
Leaf area index[c] (LAI)	8.3
Basal area (m^2 ha^{-1})	30.0
Soil texture[d]	SC-SCL[e]
Average rooting depth (cm)[d]	32.3 ± 9.6
Soil pH[d]	4.1 ± 0.09

[a] BF = balsam fir, BS = black spruce, WB, white birch, TA = trembling aspen.
[b] PCT = pre-commercially thinned.
[c] Based on TRAC II measurements (LeBlanc et al., 2002).
[d] Values are based on six soil pits.
[e] SC = sandy clay, SCL = sandy clay loam, determined by sedimentation (Bourque et al., 2006).

for 30-min averaging times. A co-ordinate rotation of wind vectors was used in the calculation of fluxes following procedures described in Tanner and Thurtell (1969).

2.2. *Model formulation*

To explore the impact of various modifications to the GFM on NEP calculations, model development will be conducted in an incremental fashion. Each model modification will be evaluated as to its performance by (i) comparing modelled results with field measurements of NEP, and (ii) quantifying modelling efficiencies (ME). Model development begins with Eqs. (11) and (12) provided in Xing et al. (2007), namely

$$\mathrm{NEP} = \sum_{i=1}^{n} \mathrm{NEP}_{\max}\{1 - L_{\mathrm{sun}}[i]\exp[-\alpha(\mathrm{PAR}_{\mathrm{sun}}[i] - \Gamma)] - L_{\mathrm{shade}}[i]\exp[-\alpha(\mathrm{PAR}_{\mathrm{shade}}[i] - \Gamma)]\}\frac{\mathrm{LAI}}{n}, \quad (1)$$

where $\mathrm{NEP}_{\max}$ (μmol CO_2 m^{-2} s^{-1}) is the maximum NEP per unit leaf area index (LAI, m^2 m^{-2}), $L_{\mathrm{sun}}[i]$ and $L_{\mathrm{shade}}[i]$ are the sunlit and shade leaf fraction in the ith canopy layer, "n" is the number of canopy layers ($n = 4$; Xing et al., 2007; De Pury and Farquhar, 1997), Γ the light compensation point (μmol m^{-2} s^{-1}), α the parameter which defines the photosynthetic efficiency (μmol^{-1} m^2 s^1), and $\mathrm{PAR}_{\mathrm{sun}}$ and $\mathrm{PAR}_{\mathrm{shade}}$ are modelled photosynthetically active radiation (μmol m^{-2} s^{-1}) absorbed by sunlit and shaded leaves based on measured PAR, respectively. Eq. (1) is derived by incorporating a new light-interception representation in Landsberg's equation [refer to Xing et al. (2007), for additional information]. Here, Eq. (1) constitutes as Model 0 for this paper. Each successive change will generate a new model (i.e., Models 1–3). Modifications and resultant model formulations are described below.

2.2.1. *Model 1*

To address daytime air temperature effects on NEP, a temperature response factor [$f(T)$] is multiplied to $\mathrm{NEP}_{\max}$ in Model 0, yielding

$$\mathrm{NEP} = \sum_{i=1}^{n} \mathrm{NEP}_{\max} f(T)\{1 - L_{\mathrm{sun}}[i]\exp[-\alpha(\mathrm{PAR}_{\mathrm{sun}}[i] - \Gamma)] - L_{\mathrm{shade}}[i]\exp[-\alpha(\mathrm{PAR}_{\mathrm{shade}}[i] - \Gamma)]\}\frac{\mathrm{LAI}}{n} \quad (2)$$

where $f(T)$ is defined as a function of $f(T_0)$ and $f(T_1)$ (Landsberg and Waring, 1997), i.e.,

$$f(T) = \begin{cases} f(T_0), & \text{if } T_a < T_{\mathrm{opt}} \\ 1, & \text{if } T_a = T_{\mathrm{opt}} \\ f(T_1)f(T_0), & \text{if } T_a \geq T_{\mathrm{opt}} \end{cases} \quad (3)$$

$$f(T_0) = \frac{1}{\exp[(T_0 - T_{\mathrm{opt}})^2/K_{\mathrm{rt}}]}, \quad (4)$$

and

$$f(T_1) = \left(\frac{T_a - T_{\min}}{T_{\mathrm{opt}} - T_{\min}}\right)\left(\frac{T_{\max} - T_a}{T_{\max} - T_{\mathrm{opt}}}\right)^{(T_{\max} - T_{\mathrm{opt}})/(T_{\mathrm{opt}} - T_{\min})} \quad (5)$$

where T_a (°C) is the air temperature, T_{opt} (°C) is the optimum air temperature for photosynthesis (set at 17.5 °C for BF), K_{rt} is a equation parameter which is used to adjust the slope of temperature curve with values ranging from 100 to 1200, and $T_{\max}$ (°C) and $T_{\min}$ (°C) are the air temperatures for which photosynthetic activity ceases. Here, $T_{\max}$ and $T_{\min}$ are set to 35 and 0 °C, respectively.

2.2.2. *Model 2*

Theoretically, plant respiration can be partitioned into two components (Thornley and Johnson, 1990), one proportional to the growth rate of the aboveground biomass (growth respiration) and the second proportional to the dry mass of plants (maintenance respiration). In the design of the model, we do not differentiate respiration components such as stem and foliage respiration because of the difficulties and uncertainties associated with these respiration terms in model parameterization. We use a single canopy-respiration term to cover all tree-related respiration, which we define as a function of air temperature.

Incorporation of ecosystem respiration in Model 0 gives

$$\mathrm{NEP} = \sum_{i=1}^{n} \mathrm{GEP}_{\max}\{1 - L_{\mathrm{sun}}[i]\exp[-\alpha(\mathrm{PAR}_{\mathrm{sun}}[i] - \Gamma)] - L_{\mathrm{shade}}[i]\exp[-\alpha(\mathrm{PAR}_{\mathrm{shade}}[i] - \Gamma)]\}\frac{\mathrm{LAI}}{n} - R_{\mathrm{ec}}, \quad (6)$$

where R_{ec} (μmol CO_2 m^{-2} s^{-1}) is the ecosystem respiration ($=R_c + R_s$) accounting for CO_2 fluxes associated with plant (foliage + branch + stem) respiration, dead tree and forest floor decomposition, soil respiration, and other above-ground CO_2-release mechanisms. Note here we use $\mathrm{GEP}_{\max}$ instead of $\mathrm{NEP}_{\max}$ [as in the earlier equations, Eqs. (1) and (2)] because we have explicitly separated ecosystem respiration (R_{ec}) from the photosynthetic component of the model. Eqs. (1) and (2) incorporate the effects of R_{ec} implicitly.

Here, R_c (μmol CO_2 m^{-2} s^{-1}) is the bulk canopy respiration defined as

$$R_c = \frac{R_{c\,\max}}{1 + \exp[-R_{c\beta}(T_a - R_{\mathrm{copt}})]} \quad (7)$$

where $R_{c\,\max}$ (μmol CO_2 m^{-2} s^{-1}) is the maximum canopy respiration, $R_{c\beta}$ ($^\circ C^{-1}$) is an equation parameter with values ranging between 0.01 and 0.999, and R_{copt} (°C) is an equation parameter with values ranging between 15 and 25.

R_s is soil respiration defined as (Lloyd and Taylor, 1994; Gu et al., 1999; Lavigne, 2003):

$$R_s = R_{s\,\max}\exp\left[R_{s\alpha}\left(R_{s\beta} - \frac{1}{T_s - 227.13}\right)\right] \quad (8)$$

where $R_{s\,\max}$ (μmol CO_2 m^{-2} s^{-1}) is the maximum soil respiration (defaulted to 2.26 μmol m^{-2} s^{-1}), T_s (°C) the soil temperature (in K), and $R_{s\alpha}$ (°C) and $R_{s\beta}$ (°C) are equation parameters set to 308 (Gu et al., 1999) and 0.017825, respectively. In this paper, equation parameters are set to constant values, but under normal gap filling equation parameters may be optimized to any value within their specified ranges, given appropriate NEP target values.

2.2.3. Model 3

Model 3 incorporates both changes [i.e., $f(T)$ and R_{ec}], giving:

$$\mathrm{NEP} = \sum_{i=1}^{n} \mathrm{GEP}_{max} f(T)\{1 - L_{sun}[i] \exp[-\alpha(\mathrm{PAR}_{sun}[i] - \Gamma)] - L_{shade}[i] \exp[-\alpha(\mathrm{PAR}_{shade}[i] - \Gamma)]\} \frac{\mathrm{LAI}}{n} - R_{ec}. \quad (9)$$

2.2.4. Model parameterization and fitting

Iterative numerical methods, such as Levenberg–Marquardt and Nelder–Mead Simplex method, are frequently used in non-linear model parameterization. This is accomplished by minimizing the difference between the model's results and target data (observations), provided in terms of the weighted sum of squares and expressed as

$$\chi^2 = \sum \frac{(P_j - O_j)^2}{Er^2}, \quad (10)$$

where O_j is the target value, P_j the calculated value, Er is the uncertainty associated with the data values predetermined by the user, and j represents a specified target data-versus-prediction data pair. Fitted parameters for the various models are listed in Table 2.

2.3. Model performance

To evaluate model performance, we use model efficiency (ME) as the main performance criterion, i.e.:

$$\mathrm{ME} = 1 - \frac{\sum_{i=1}^{N}(P_i - O_i)^2}{\sum_{i=1}^{N}(|P'_i| + |O'_i|)^2} \quad (11)$$

where P_i and O_i are the corresponding predicted and observation values, $\bar{O}$ is the mean of all the observation values and $P'_i = P_i - \bar{O}$, and $O'_i = O_i - \bar{O}$ (Willmott, 1981; Leuning et al., 1998). ME-values range from [0,1] as agreement between predicted values and observations change from no agreement (ME = 0) to perfect agreement (ME = 1; Figuerola and Mazzeo, 1997).

2.4. Analysis platform

ModelMaker v. 3.0 (Cherwell Scientific Ltd., Oxford, UK) provides an object-oriented modelling platform for the development, parameterization, and testing of Model 1 through Model 3. Data analysis in this paper was performed using the statistical functions in MS Excel.

3. Results and discussion

3.1. Weather conditions over the 34-day evaluation period

Fig. 1a provides time series of direct and diffuse PAR during a 34-day evaluation period (DOY 161–196 or 9 June–14 July 2004). Fig. 1b gives the corresponding temporal variation in other environmental factors, including air temperature (T_a), relative humidity (RH), and soil temperature (T_s). For the 34-day period,

Table 2 – Parameter values derived from model parameterization using TableCurve 2D™ v. 5.1 [Systat Software Inc. (SSI), San Jose, CA, USA] for Landsberg's equation (Xing et al., 2007) and ModelMaker™ v. 3.0 (Cherwell Scientific Ltd. Oxford, UK) for Model 0 [in Xing et al. (2007)] through to Model 3

Model	Light-related			Temperature-related				Soil-related			Model Fit		Note
	A	Γ	GEP_{max}[a]	K_{rt}	$R_{c\,max}$	$R_{c\beta}$	$R_{c\,opt}$	$R_{s\,max}$	$R_{s\alpha}$	$R_{s\beta}$	r^2	F	
Landsberg's equation	0.002866	102.1	1.49	–	–	–	–	–	–	–	0.71	–	Xing et al. (2007)
Model 0	0.005676	13.7	4.86	–	–	–	–	–	–	–	0.72	1807	Xing et al. (2007)
Model 1	0.004663	14.3	6.47	447.6	–	–	–	–	–	–	0.77	1203	New model
Model 2	0.005438	0.1	5.61	–	10.0	0.52	25	2.26	308	0.017	0.75	1187	New model
Model 3	0.0047367	0.0	6.62	1199	1	0.84	25	2.26	308	0.017	0.78	559	New model

In this paper, p-values <0.001 for all estimated parameter values.

[a] GEP_{max} is a parameter defining the maximum gross ecosystem productivity (GEP) at optimal growing conditions; NEP_{max} in Landsberg's equation and variants of the equation defines maximum net ecosystem productivity and includes the effects of ecosystem respiration. For Landsberg's equation, NEP_{max} is based on a unit LAI, while for other equations and GEP_{max} in the new equations where ecosystem respiration is explicit) the values are based on LAI/4, where 4 represents the number of layers in the canopy. α is a parameter which determined a light use efficiency, Γ is the parameter determining light compensation point, K_{rt} is the parameter to determine temperature influence on photosynthesis, $R_{c\,max}$, $R_{c\beta}$ and R_{copt} are the parameters determining the maximum canopy respiration, a shape factor for the canopy respiration function, and the reference temperature at which canopy respiration is highest, $R_{s\,max}$, $R_{s\beta}$, and $R_{s\alpha}$ are parameters specifying maximum soil respiration, a shape factor for the soil respiration function, and a shape factor for the soil respiration curve. Model 0 is described by Eq. (1); Model 1 by Eq. (2), Model 2 by Eq. (6), and Model 3 by Eq. (9).

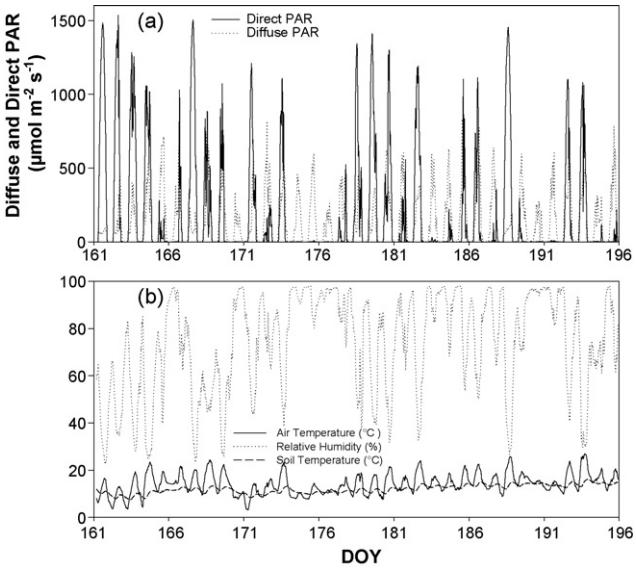

Fig. 1 – Time series of environmental conditions: (a) direct and diffuse PAR and (b) air temperature, relative humidity, and soil temperature for DOY 161–196 (9 June–14 July 2004). Data was collected at the NWL_BF FCRN flux site.

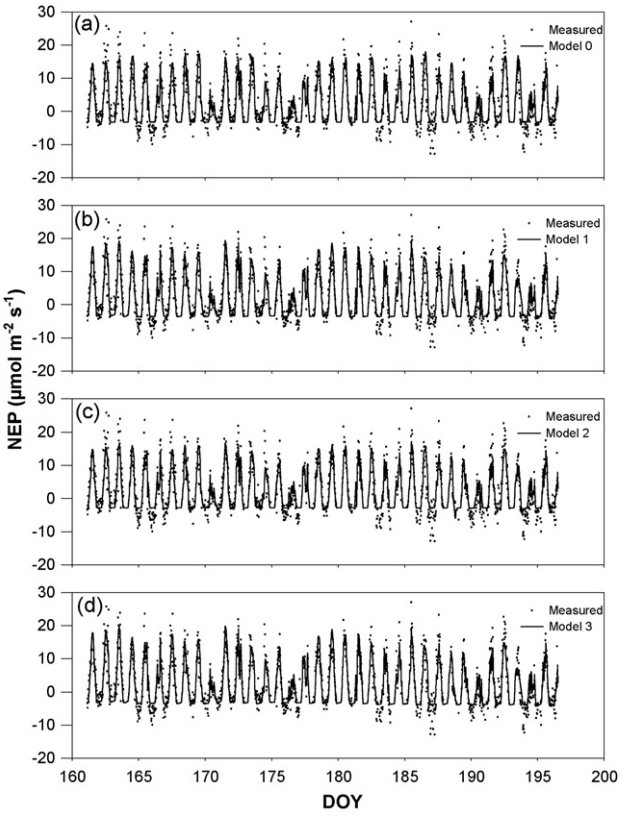

Fig. 2 – Measured vs. modelled time series of NEP for the four models (a = Model 0 through to d = Model 3) over DOY 161–196, 2004.

total PAR, direct PAR, and diffuse PAR averaged to 330, 185, and 145 $\mu mol\,m^{-2}\,s^{-1}$, respectively. Average daytime diffuse-to-total PAR ratio for the 34-day period was 44%; as a result of 14 very cloudy days, 10 intermediate cloudy days, and 10 clear days. Among the 1700 PAR measurements used in model development (accounting for both daytime and nighttime measurements) (i) 12% had values above 1000 $\mu mol\,m^{-2}\,s^{-1}$, (ii) 14%, with values between 500 and 1000 $\mu mol\,m^{-2}\,s^{-1}$, (iii) 25%, with values between 100 and 500 $\mu mol\,m^{-2}\,s^{-1}$, and (iv) the remaining, with values <100 $\mu mol\,m^{-2}\,s^{-1}$. Air temperature (T_a) varied between 3 and 27 °C, with an average of 14.3 °C over the 34-day period, as a result of 11 warm days (peak $T_a > 20$ °C) and 5 cool days (peak $T_a < 5$ °C). RH varied from 20 to 98% with a 34-day average of 75%, as a result of 11 comparatively dry days, with RH < 40%. Soil temperature (T_s) varied from 7.4 to 16.2 °C with a 34-day average of 12.0 °C. Volumetric soil water content (SWC, in %) demonstrated very little variation over the 34-day period with values ranging between 7.0 and 11.6%, with an average of 9%. This dataset provided an ideal range of weather conditions for the evaluation of Landsberg's equation (Xing et al., 2007), and Model 0 [Eq. (1)] through to Model 3 [Eq. (9)].

3.2. *Model performance*

3.2.1. *Model 1 [Eq. (2)]*

In comparison to Model 0 (Fig. 2a), Model 1 (Fig. 2b) offered some improvement in the representation of peak values in NEP. On a day-by-day basis, Model 1 performed better than Model 0, particularly, on DOY 189, when direct PAR was high (1500 $\mu mol\,m^{-2}\,s^{-1}$) and DOY 175, when diffuse PAR was intermediate (436 in $\mu mol\,m^{-2}\,s^{-1}$) and direct PAR was low (<20 $\mu mol\,m^{-2}\,s^{-1}$). No obvious improvement was apparent for nighttime prediction of NEP.

Regressions of measurement-to-prediction pairs (Fig. 3) indicated that Model 1 (Fig. 3c) provided a better representation of measured NEP ($r^2 = 0.77$, regression of slope of 0.99) than did either Landsberg's equation (Fig. 3a, $r^2 = 0.71$, slope = 0.99) or Model 0 (Fig. 3b, $r^2 = 0.72$, slope = 0.99). With temperature control in Model 1, modelled peak values climbed from 12 $\mu mol\,m^{-2}\,s^{-1}$ using Model 0, to 18 $\mu mol\,m^{-2}\,s^{-1}$. Although Model 1 provided improvement over Model 0, it nonetheless underestimated actual peak values (maximum at 24 $\mu mol\,m^{-2}\,s^{-1}$) by about 30%, in the worst instances. The sharp edge to the left-hand side of the data field in Fig. 3a–c coincides with poor nighttime prediction of NEP (also see Fig. 2).

Model 1 gave slightly better results than Model 0 (Figures 3a and b, 4a and b, and 5a and b) as Model 1 incorporated the interaction between light availability and air temperature in its influence on NEP. Improvement occurred when PAR was at or above the plants light saturation point, at ~600 $\mu mol\,m^{-2}\,s^{-1}$ (Fig. 4). This was reasonable; because beyond this point, PAR had a reduced control on NEP and any increments in NEP were likely associated with other controlling variables, like air temperature (Fig. 5a and b).

Modelled NEP-air temperature relationship in Fig. 5c (for Model 1) more closely replicated the dispersion pattern (unimodal distribution) illustrated in the measured data (Fig. 5f), especially for daytime NEP values >0.0 $\mu mol\,m^{-2}\,s^{-1}$ compared to results generated with Landsberg's equation or Model 0.

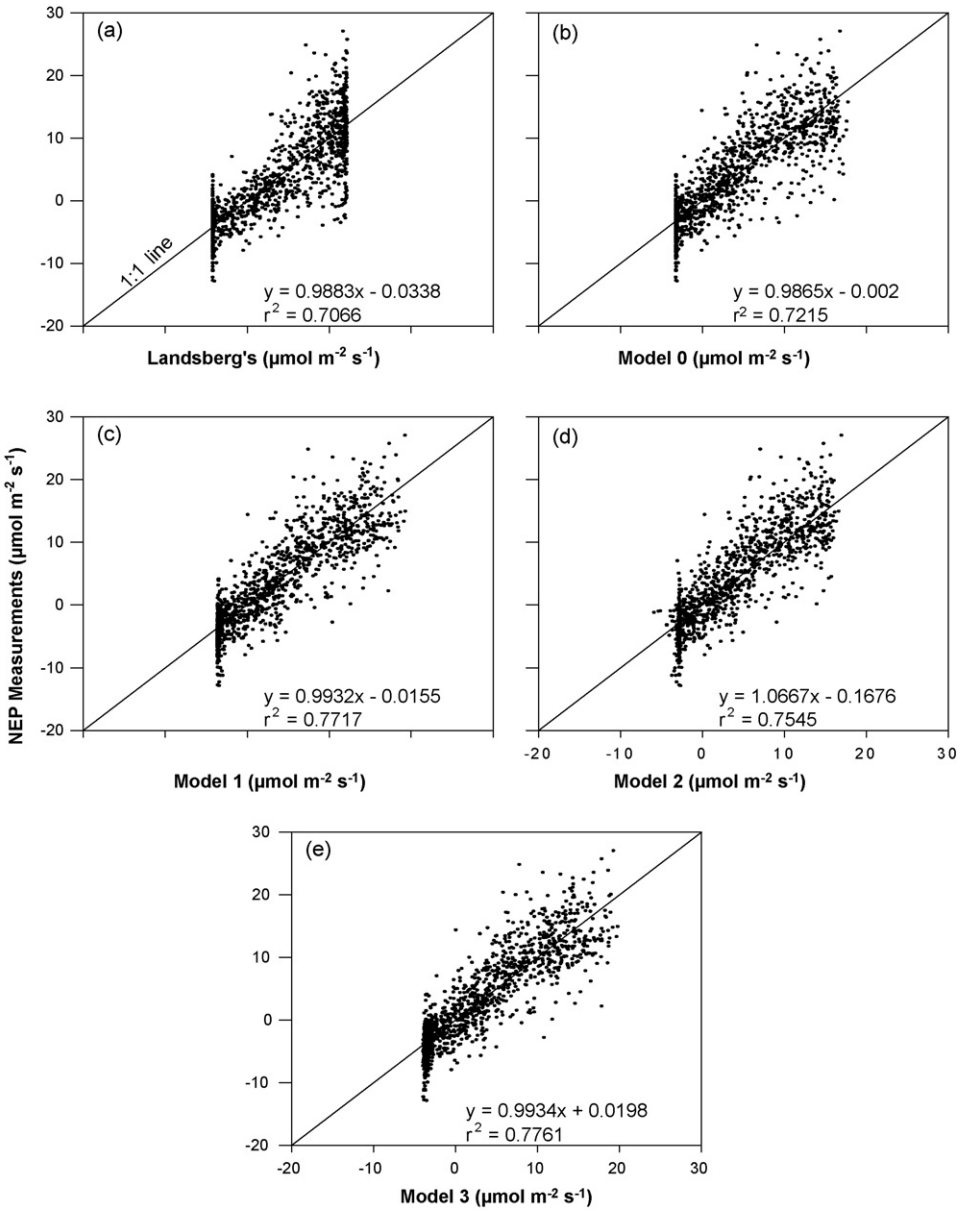

Fig. 3 – Regression analysis applied to modelled-vs.-measurment data pairs, with modelled values derived from Landsberg's equation (a) and the four models [Model 0–3; Eqs. (1), (2), (6), and (9); graphs (b–e)]. The *x*-axis of each graph is associated with the modelled values and the *y*-axis, to the measured values. In each case, a regression equation is fitted to the data points to determine the best overall agreement between modelled and measured values. For complete agreement, all data points would align exactly along the 1:1 correspondence (diagonal) line. Mean deviation from the 1:1 line is expressed in a regression slope different from 1.0 and a *y*-intercept, different from 0.0.

Implementation of the changes in Model 1 caused two major improvements in data representation, namely (i) overestimates of NEP produced with Landsberg's equation and Model 0 (Fig. 6a and b) near the biological limits of air temperature (i.e., $T_a \leq 5\,^{\circ}C$ or $T_a \leq 25\,^{\circ}C$), were considerably reduced, and (ii) peak NEP values ($\sim 18\,\mu mol\,m^{-2}\,s^{-1}$) were generally made to coincide with air temperatures in the optimal temperature range, i.e., 15–20 °C, as displayed in the measured data (Fig. 5f). Fig. 6 provides a day-to-day assessment of daily ME values for the four models. ME values for Model 1 were consistently higher than those of Model 0 by at least 3% on average, with a range of 0–18% for the different days. The greatest deviation occurred on DOY 176, 184, 188 and 193 (Fig. 6), when higher-than-optimum air temperatures (>17.5 °C) caused a reduction in NEP.

As Thornley and Johnson (1990) pointed out, the effects of temperature on biological systems have long been a source of confusion and controversy to plant- and eco-physiologists because temperature may operate as a single rate-limiting factor or may operate as a factor with multiple-phase dependencies. In this work, temperature was considered as a single rate-limiting factor of GEP_{max}, as it is easiest to imple-

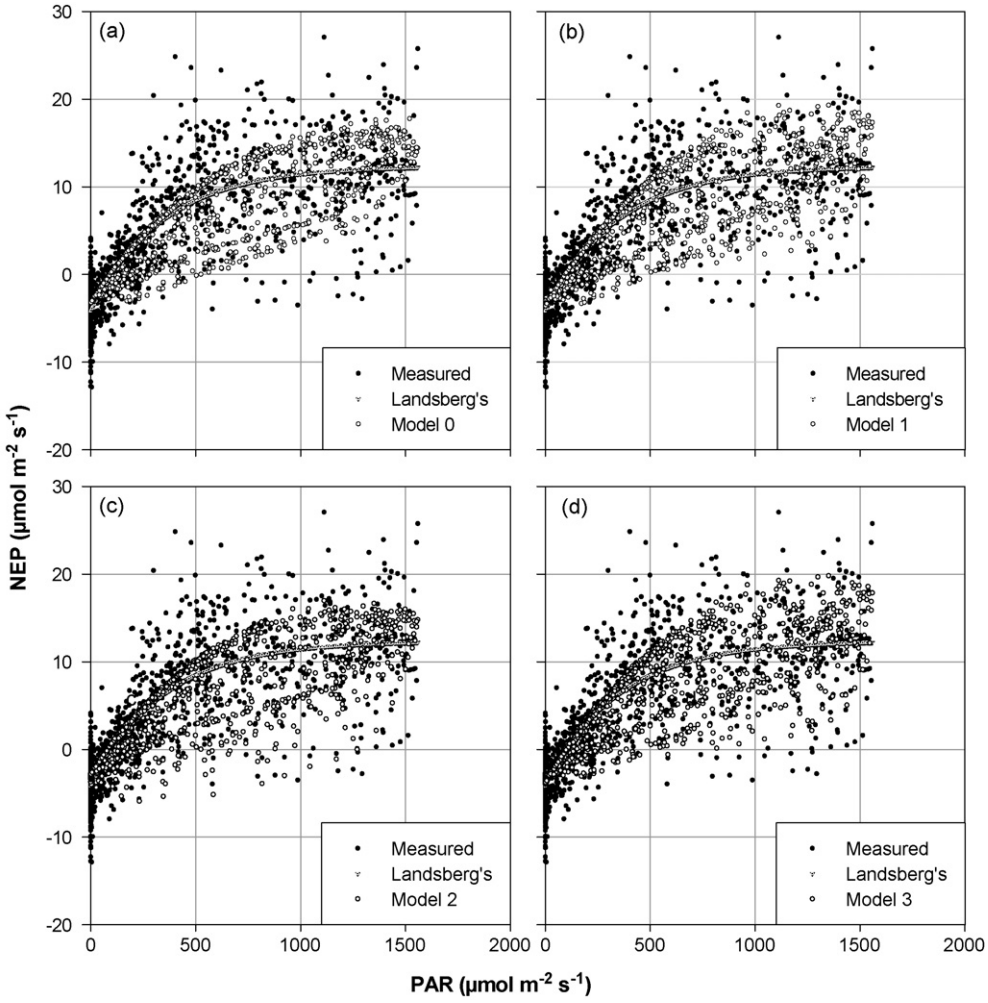

Fig. 4 – Measured and modelled variation in NEP as a function of PAR. Modelled NEP is based on Landsberg's equation (mean representation) and the four models (Model 0 through Model 3). Light saturation occurs at the point the light-response curve (derived with Landsberg's equation) reaches the smallest increment in NEP (i.e., $\Delta NEP/\Delta PAR \approx 0$) despite linear increases in PAR.

ment. Unsatisfactory performance of Model 1 with nighttime NEP may be an indication of air temperatures' multiple-phase effects in light harvesting, CO_2 fixation, and biological activity in soils. Model 1, in its current form, may not provide satisfactory estimates of NEP when air temperatures diverge from the mean temperature during the study period.

3.2.2. *Model 2 [Eq. (6)]*

Fig. 2c provides modelled and measured day-to-day variation in NEP over the 34-day evaluation period (DOY 161–196). Fig. 3d displays the same NEP data as a function of predicted values obtained with Model 2. In general, Model 2 did not improve results from those of Model 0. As anticipated, incorporation of R_{ec} in model formulation had nominal effect on the daytime temperature-response portion (Fig. 6c and f) of the dispersion pattern (Fig. 5d), but had greater effect on the respiration-dominated (nighttime) portion of NEP (Fig. 4c). Fig. 4c suggests that the maximum modelled NEP was bounded by an upper limit of $\sim$15 $\mu mol\,m^{-2}\,s^{-1}$, underestimating actual peak values ($\sim$25 $\mu mol\,m^{-2}\,s^{-1}$) by about 50%. A slight reduction in modelled NEP was observed to occur when air temperatures exceeded 20 °C, a reduction not produced with Model 0 (corresponding ME-values are shown in Fig. 6).

3.2.3. *Model 3 [Eq. (9)]*

In general, Model 3 provided better predictions of NEP (Fig. 2d), except for a slight overestimation on DOY 162, 179, and 180. In this simulation, parameters for soil respiration [in Eq. (8)] were kept constant, as soil-respiration data were not available for this study. Scatter-diagrams of modelled-versus-measured NEP data pairs in Fig. 3e provided reasonable agreement, except for nighttime values. Maximum NEP attained on any given day was $\sim$20 $\mu mol\,m^{-2}\,s^{-1}$.

Light-response (Fig. 4d) of modelled NEP provided a reasonable agreement with the low NEP-values across the entire PAR range (i.e., 0–1500 $\mu mol\,m^{-2}\,s^{-1}$). High NEP values with high PAR values (>1000 $\mu mol\,m^{-2}\,s^{-1}$) were generally well presented. However, with PAR values in the range of 300–600 $\mu mol\,m^{-2}\,s^{-1}$, Model 3 generally underestimated NEP.

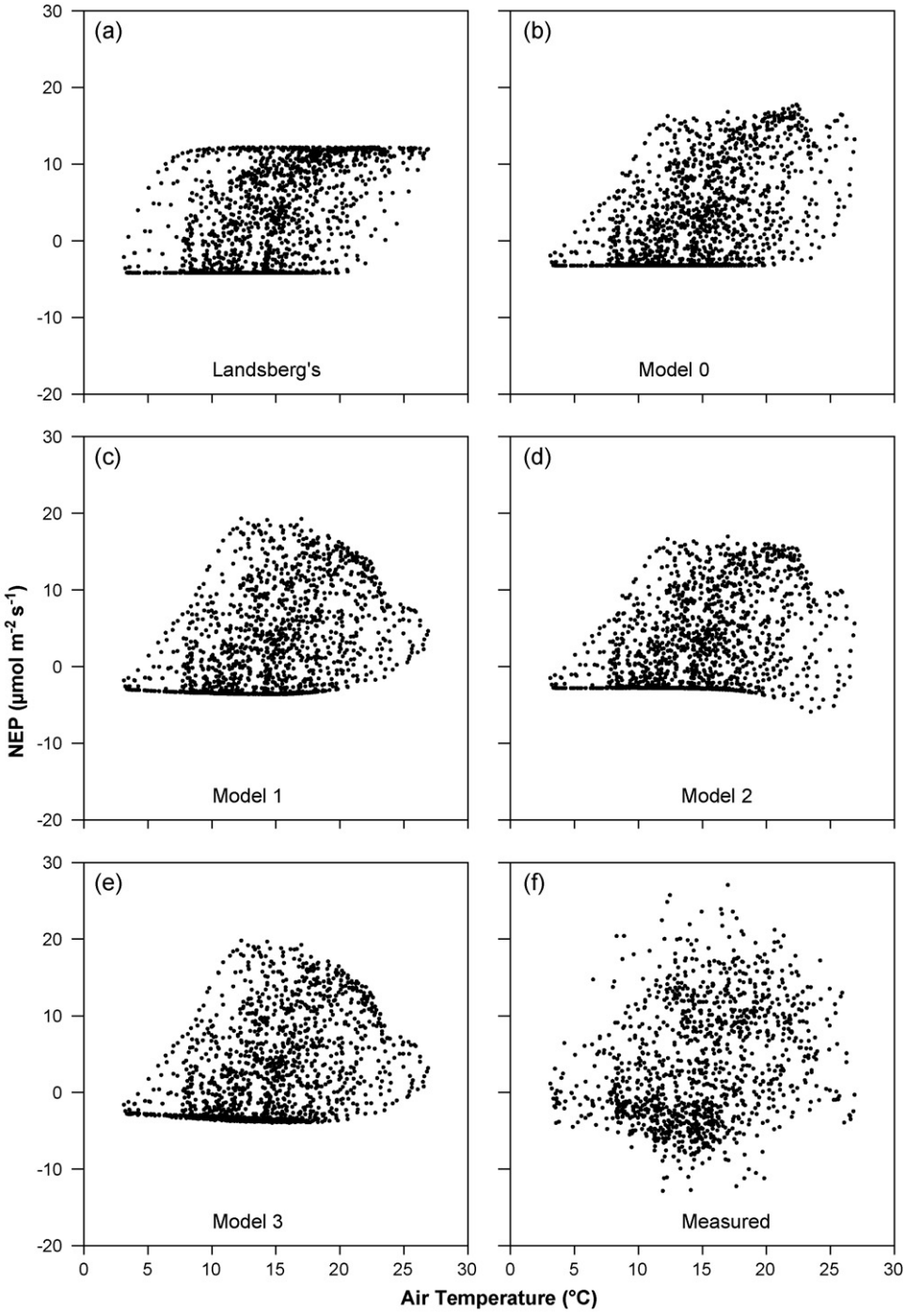

Fig. 5 – Modelled (a–e) and measured (f) NEP as a function of air temperature. Modelled values are based on Landsberg's equation (a) and the four models (Model 0 through Model 3; graphs (b–e)).

This underestimation was likely caused by a bias in parameter definition associated with an imbalance in the number of clear days used in model parameterization.

Response of modelled NEP to air temperature (Fig. 5e) was similar to the actual response (Fig. 5f) for NEP > 0.0 μmol m^{-2} s^{-1}. Monitoring NEP with eddy-covariance techniques often yield unrepresentative values at night when the atmosphere is stable, wind velocities are low and in-canopy and trunk-space ventilation is reduced. Occasional releases of CO_2-enriched air from below the canopy at night are generally observed as extremely high peaks. Such peaks are very difficult to reproduce with models, as the controlling variables often operate independently and at a different spatial resolution from local processes of photosynthesis (C uptake) and respiration. Statistical examination of the data suggested that the model produced only 11% estimate error, when $T_a < 10\,^{\circ}C$, and −13% bias, when T_a ranged between 10 and 20 °C (refer to Fig. 6e and f).

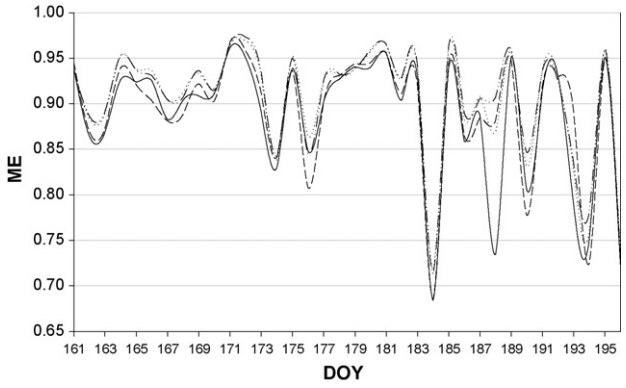

Fig. 6 – Modelling efficiencies (ME) for Model 0 through to Model 3 as a function of DOY. ME values are given here as daily averages of half-hourly values.

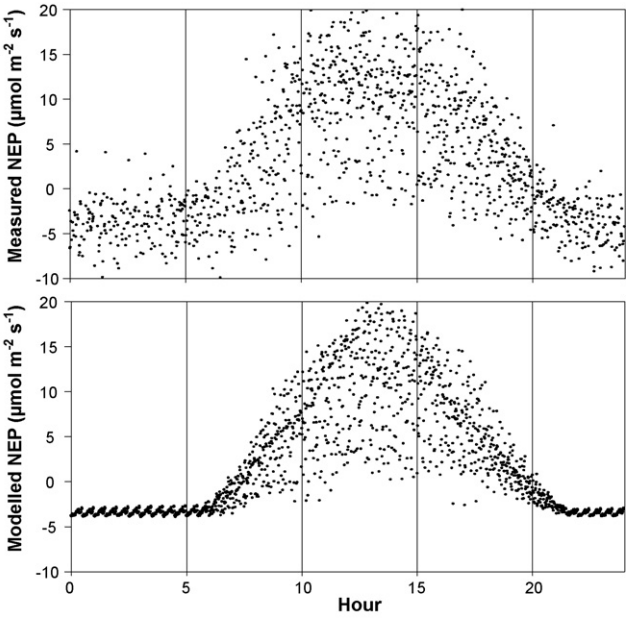

Fig. 7 – Diurnal variation of measured (a) and modelled (b) NEP.

Model efficiency values for Model 3 (Fig. 6) were generally higher than those produced for the other models (i.e., Landsberg's equation + Model 0–2), except for DOY 184 and 196. The poorer representation during these 2 days may suggest that other environmental factors, beyond the ones considered in this paper (like RH and SWC), may have been involved in the control of NEP.

Our results clearly demonstrated that Model 3 performed the best among the models investigated with respect to light and temperature response, day-to-day variation in NEP, and ME-values produced (Fig. 6). For further examination of the day-to-day response of Model 3, measured and modelled NEP values were plotted as a function of time (Fig. 7). Time response of the model was generally good for the daytime period and, as expected, poor for the nighttime period. Despite the large variation in actual nighttime values, the model represented average NEP for nighttime conditions reasonably well.

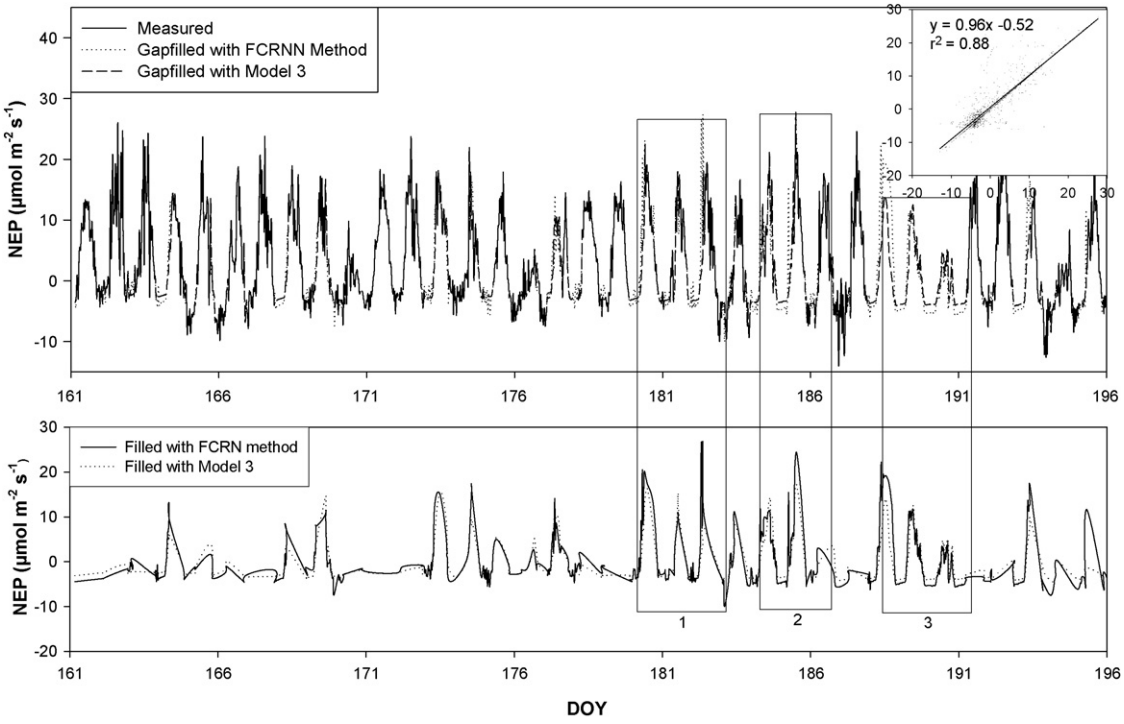

Fig. 8 – 34-day time series of NEP of actual measurements with gaps and gap filled with the FCRN-adopted methodology and Model 3 (a). The inset to graph (a) shows the regression between the gap-filled NEP values using FCRN's recommended methodology (*x*-axis) and Model 3 (*y*-axis). The boxes indicate major gaps in the measurement data stream. The lower graph (b) shows the major data gaps and performance of each gap-filling methodology, and each peak indicates a gap.

3.3. *Gap-filling comparisons*

To further test Model 3, its results were compared with the results from the FCRN-recommended gap-filling methodology of Amiro et al. (2005). In general, gap filling with both methodologies were in very good agreement with one another and with the measured data, yielding an r^2-value of 0.88 and regression slope of 0.96; The FRCN methodology, however, predicted on average 13% higher values than did Model 3 (Fig. 8a). Greatest discrepancy between the two-modelled results occurred when the dataset had the greatest number of missing consecutive observations.

In the first identified segment of Fig. 8a, both methods give very similar results. In the second segment (Fig. 8a), gap filling with both methods was generally very good for the first 2 days, but significant discrepancies were observed on the third day. In the third segment (Fig. 8a) greatest discrepancy occurred on the first day. These discrepancies may be caused by (i) model structure differences; the FCRN-adopted methodology uses $\mathrm{NEP} = aQb/(Q+b) - R$[4] as its core equation, which was found to give similar results to the core equation of Model 3 (i.e., Landsberg's equation), although slight differences were observed (Xing et al., 2007). Because the FCRN-adopted methodology does not explicitly consider canopy light differentiation with sun position and light penetration properties through a vertically stratified canopy, Model 3 predictions may slightly differ from those generated with the FCRN method when direct PAR dominates; (ii) Model 3 uses dynamic model fitting and auto-parameterization to calculate NEP from strings of instantaneous values of PAR and T_a, while the FCRN-adopted methodology uses the diurnal pattern in the previous 5 days as an indication of future trends in NEP. This approach may cause incorrect predictions, especially if weather conditions during the previous 5 days and the day(s) to be gap filled are significantly different; and (iii) large data gaps may produce inferior predictions when the gap-filling procedure is far away from the reference information upstream.

4. Conclusions

- Generally, Model 1 showed a significant improvement during the period when $\mathrm{PAR} > 1000\,\mu\mathrm{mol\,m^{-2}\,s^{-1}}$.
- Model 2 obtained a nominally better nighttime prediction of NEP than Model 0 because its formulation captured the diurnal variations of canopy and soil respiration. However, it did not provide much improvement to daytime estimates of NEP compared to Model 0.
- Model 3 provided an obvious improvement over Model 0 through Model 2 for various weather conditions.
- Nighttime NEP predictions with Model 3 (the final version of the GFM) remain poor. Both uncertainties embedded in nighttime NEP measurements and model structure may be responsible for this poor performance. If hourly averaged soil respiration data were available and used in model fitting, a better nighttime representation of NEP could most likely be obtained with Model 3.
- Gap-filling results generated with Model 3 and the FCRN-adopted methodology showed reasonable agreement ($r^2 = 0.88$), although some discrepancies existed between results. Results from the FCRN methodology were generally higher than those from Model 3 by about 13%. Model 3 does not have the constraints associated with gap size and gap position as the FCRN-method seems to have.

[4] a and b are constants based on values derived from annual datasets, and Q represents PAR in the equation.

Acknowledgements

This paper could not have been completed without financial support from the Natural Science and Engineering Council of Canada (NSERC), BIOCAP Canada Foundation, and the Canadian Foundation of Climate and Atmospheric Sciences (CFCAS), through the Fluxnet-Canada project. We are also grateful to the Canadian Forest Service—Atlantic Forest Centre, Fredericton, New Brunswick for financial and logistical support of this research.

REFERENCES

Amiro, B.D., Bar, A.G., Black, T.A., Iwashita, H., Kljun, N., McCaughey, J.H., Morgenstern, K., Murayama, S., Nesic, Z., Orchansky, A.L., Saigusa, N., 2005. Carbon, energy and water fluxes at mature and disturbed forest sites, Saskatchewan, Canada. Agric. For. Meteorol. 136, 237–251.

Bassow, S.L., Bazzaz, F.A., 1998. How environmental conditions affect canopy leaf-level photosynthesis in four deciduous tree species. Ecology 79, 2660–2675.

Bourque, P.-A., Lehnert, S., Xing, Z., Meng, F.-R., Swift, D.E., 2006. Site influences on net ecosystem productivity in managed *Abies Balsamea* stands. In: Proceedings of the International Conference on Regional Carbon Budgets, pp. 25–31.

Caemmerer, S.V., 2000. Modelling C_3 photosynthesis. In: Biochemical Models of Leaf Photosynthesis. CSIRO Publishing, Collingwood, Vic, pp. 29–70.

Cai, T.B., Dang, Q.L., 2002. Effects of soil temperature on parameters of a coupled photosynthesis-stomatal conductance model. Tree Physiol. 22, 819–827.

Chen, J.M., Liu, J., Cihlar, J., Goulden, M.L., 1999. Daily canopy photosynthesis model through temporal and spatial scaling for remote sensing applications. Ecol. Model. 124, 99–119.

Chen, J., Falk, M., Euskirchen, E., Paw, U.K.T., Suchanek, T., Ustin, S., Bond, B.J., Brosofske, K.D., Phillips, N., Bi, R.C., 2002. Biophysical controls of carbon flows in three successional Douglas-fir stands based on eddy-covariance measurements. Tree Physiol. 22, 169–177.

Coleman, D.C., Hunter, M.D., Hutton, J., Pomeroy, S., Swift Jr., L., 2002. Soil respiration from four aggrading forested watersheds measured over a quarter century. For. Ecol. Manage. 157, 247–253.

Coursolle, C., Margolis, H.A., Barr, A.G., Black, T.A., Amiro, B.D., McCaughey, J.H., Flanagan, L.B., Lafleur, P.M., Roulet, N.T., Bourque, C.P.-A., Arain, M.A., Wofsy, S.C., Dunn, A., Morgenstern, K., Orchansky, A.L., Bernier, P.Y., Chen, J.M., Kidston, J., Saigusa, N., Hedstrom, N., 2006. Late-summer carbon fluxes from Canadian forests and peatlands along an east–west continental transect. Can. J. For. Res. 36 (3), 783–800.

De Pury, D.G.G., Farquhar, G.D., 1997. Simple scaling of photosynthesis from leaves to canopies without the errors of big-leaf models. Plant Cell Environ. 20, 537–557.

Ecological Classification Working Group, 2003. Our landscape heritage: the story of ecological classification in New Brunswick. N. B. Dept. Nat. Resources and Energy, Fredericton, NB, Canada (CD-ROM).

Farquhar, G.D., 1980. A biochemical model of photosynthetic CO_2 assimilation in leaves of C_3 species. Planta 149, 78–90.

Figuerola, P.I., Mazzeo, N.A., 1997. An analytical model for the prediction of nocturnal and dawn surface temperatures under calm, clear sky conditions. Agric. For. Meteorol. 85, 229–237.

Grant, R.F., 2004. Modelling topographic effects on net ecosystem productivity of boreal black spruce forests. Tree Physiol. 24, 1–18.

Grant, R.F., Goulden, M.L., Wofsy, S.C., Berry, J.A., 2001. Carbon and energy exchange by a black spruce-moss ecosystem under changing climate: testing the mathematical model *ecosys* with data from the BOREAS experiment. J. Geophys. Res.-Atmos. 106, 33605–33621.

Grant, R.F., Arain, M.A., Arora, V., Barr, A., Black, T.A., Chen, J., Wang, S., Yuan, F., Zhang, Y., 2005. Intercomparison of techniques to model high temperature effects on CO_2 and energy exchange in temperate and boreal coniferous forests. Ecol. Model. 188, 217–252.

Gu, L.H., Shugart, H.H., Fuentes, J.D., Black, T.A., Shewchuk, S.R., 1999. Micrometeorology, biophysical exchanges and NEE decomposition in a two-story boreal forest-development and test of an integrated model. Agric. For. Meteorol. 94, 123–148.

Harley, P.C., Baldocchi, D.D., 1995. Scaling carbon-dioxide and water-vapor exchange from leaf to canopy in a deciduous forest. 1. Leaf model parametrization. Plant Cell Environ. 18, 1146–1156.

Hollinger, D.Y., Goltz, S.M., Davidson, A., Lee, J.T., Tu, K., Valentine, H.T., 1999. Seasonal patterns and environmental control of carbon dioxide and water vapour exchange in an ectonal boreal forest. Global Change Biol. 5, 891–902.

Jarvis, P.G., McNaughton, K.G., 1986. Stomatal control of transpiration scaling up from leaf to region. Adv. Ecol. Res. 15, 1–45.

Kimmins, J.P., 1987. Forest Ecology. Macmillan Publishing Company, New York.

Landsberg, J.J., Waring, R.H., 1997. A generalised model of forest productivity using simplified concepts of radiation-use efficiency, carbon balance and partitioning. For. Ecol. Manage. 95, 209–228.

Lavigne, M.B., 2003. Soil respiration responses to temperature are controlled more by roots than by decomposition in balsam fir ecosystems. Can. J. For. Res. 33, 1744–1753.

Leuning, R., 1995. A critical-appraisal of a combined stomatal-photosynthesis model for C_3 plants. Plant Cell Environ. 18, 339–355.

Leuning, R., 2002. Temperature dependence of two parameters in a photosynthesis model. Plant Cell Environ. 25, 1205–1210.

Leuning, R., Dunin, F.X., Wang, Y.P., 1998. A two-leaf model for canopy conductance, photosynthesis and partitioning of available energy. II. Comparison with measurements. Agric. For. Meteorol. 91, 113–125.

Liu, Q., Edwards, N.T., 2006. Temperature-independent diel variation in soil respiration observed from a temperature deciduous forest. Global Change Biol..

Lloyd, J., Taylor, J.A., 1994. On the temperature dependence of soil respiration. Funct. Ecol. 8, 315–323.

McMurtrie, R.E., Wang, Y.P., 1993. Mathematical models of the photosynthetic response of tree stands to rising CO_2 concentration and temperature. Plant Cell Environ. 16, 1–13.

Morgenstern, K., Black, T.A., Humphreys, E.R., Griffis, T.J., Drewitt, G.G., Cai, T., Nesic, Z., Spottlehouse, D.L., Livingston, N.J., 2004. Sensitivity and uncertainty in the carbon balance of a Pacific northwest Douglas fir forest during an El Niño/El Niña cycle. Agric. For. Meteorol. 123, 201–219.

Saxe, H., Cannel, M.G.R., Johnsen, Q., Ryan, M.G., Vourlitis, G., 2001. Tree and forest function in response to global warming. New Phytol. 149, 369–399.

Tanner, C.B., Thurtell, G.W., 1969. Sesible Heat Flux Measurements with a Yaw Sphere and Thermometer. TR Ecom 66-G22-F. Department of Soil Science, University Wisconsin, Madison, Wisconsin.

Thornley, J.H.M., Johnson, I.R., 1990. Plant and crop modelling—a mathemational approach to plant and crop physiology. Clarendon Press, Oxford.

Verseghy, D.L., 1991. Class-A Canadian land surface scheme for GCMs I, soil model. Int. J. Climatol. 11, 103–113.

Verseghy, D.L., 2000. The Canada land surface scheme (CLASS): its history and future. Atmos.-Ocean 38, 1–13.

Verseghy, D.L., McFarlane, N.A., Lazare, M., 1991. Class-A Canadian land surface scheme for GCMs II, vegetation model and coupled run. Int. J. Climatol. 13, 347–370.

Willmott, C.J., 1981. On the validation of models. Phys. Geogr. 2, 184–194.

Xing, Z., Bourque, C.P.-A., Swift, D.E., Clowater, C.W., Krasowski, M., Meng, F.R., 2005. Carbon and biomass partitioning in balsam fir (*Abies balsamea*). Tree Physiol. 25, 1207–1217.

Xing, Z., Bourque, C.P.-A., Meng, F.-R., Zha, T.-S., Cox, R.M., Swift, E., 2007. A simple net ecosystem productivity model for gap filling of tower-based fluxes: an extension of Landsberg's equation with modifications to the light interception term. Ecol. Model. 206, 250–262.

Zha, T.-S., Xing, Z., Wang, K.Y., Kellomäki, S., Barr, A.G., 2007. Total and component carbon fluxes of a Scots pine ecosystem from chamber measurements and eddy covariance. Ann. Bot. 99, 345–353.